

Observations and analysis of an urban boundary layer during extreme heat events

Gabriel Rios ^{1*}, ^{2*}, Prathap Ramamurthy ^{1, 2}, Mark Arend ^{2, 3}

1. Department of Mechanical Engineering, CUNY City College, New York, New York
2. NOAA Center for Earth System Sciences and Remote Sensing Technologies, New York, New York
3. Department of Electrical Engineering, CUNY City College, New York, New York

Corresponding author: Gabriel Rios (grios001@citymail.cuny.edu)

*** Current affiliation(s):** Department of Mechanical Engineering, CUNY City College, New York, New York; NOAA Center for Earth System Sciences and Remote Sensing Technologies, New York, New York

For submission to the Quarterly Journal of the Royal Meteorological Society.

Last updated: February 4, 2022.

¹ Abstract

2 Extreme heat presents a significant risk to human health and infrastructure in cities. Several studies
3 have been conducted in the past two decades to understand the interaction between the synoptic-scale
4 extreme heat events and local-scale urban heat island effects. However, observations of boundary layer
5 characteristics during these periods have been relatively rare. Our current understanding of boundary
6 layer dynamics is incomplete, particularly in coastal urban environments where the local climatology
7 is highly influenced by land-sea thermal gradients. Here we analyze the evolution and structure of the
8 urban boundary layer during regular and extreme heat periods. Our primary goal is to understand how
9 boundary layer dynamics during extreme heat events regulate near-surface transport of mass, momentum,
10 and heat. The analysis will also focus on how the urban surface layer interacts with the mixed layer during
11 these events. Our analysis focuses on the New York City metropolitan area and relies on observations from
12 vertical profilers (Doppler lidar, microwave radiometer) and quantities derived by analytical methods.
13 Additionally, satellite and reanalysis data are used to supplement observational data.

¹⁴ 1 Introduction

15 Extreme heat poses a major risk to life and property. The effects of extreme heat are expected to
16 impact cities especially, which presents a significant hazard for vulnerable populations and infrastructure.
17 With regards to effects on public health, studies have shown that extreme and prolonged heat increases
18 mortality and exacerbates existing health conditions in high-risk populations (Anderson and Bell, [2011](#);
19 Frumkin, [2016](#); Heaviside, Macintyre, and Vardoulakis, [2017](#); Madrigano et al., [2015](#)). With regards to
20 effects on infrastructure, studies have shown that extreme heat subjects networks critical to urban areas
21 (e.g., electrical grid, public transportation) under significant stresses and/or failure (McEvoy, Ahmed,
22 and Mullett, [2012](#); Zuo et al., [2015](#)). These events are projected to increase in frequency due to the effects
23 of climate change. Projections indicate that the impacts of future climate will cause adverse effects of
24 extreme heat to become more frequent and severe (Burillo et al., [2019](#); Forzieri et al., [2018](#); Peng et al.,
25 [2011](#)).

26 The meteorology of extreme heat events and its impacts on urban areas can be observed from the synoptic
27 and local scales. From a synoptic scale, extreme heat events are often caused by the sustained presence of
28 a high-pressure system over an area, resulting in lower wind speeds and warm air subsidence, promoting

higher surface temperatures (Black et al., 2004; Miralles et al., 2014). From a local perspective, the amplified impact of extreme heat events on cities is a result of the urban heat island (UHI) effect, which occurs as a result of the modification of land surface properties due to the built environment. The modification of surface properties has been shown to increase near-surface air temperatures due to factors such as radiation entrapment, increased heat storage, and lower evapotranspirative cooling (Chen, Yang, and Zhu, 2014; Li and Elie Bou-Zeid, 2013; Ramamurthy and Bou-Zeid, 2017; Zhao et al., 2018). Additionally, urban areas near large bodies of water experience effects from the sea breeze, which has been shown to play a moderating influence on the intensity of the UHI effect (Hu and Xue, 2016; Jiang et al., 2019; Stéfanon et al., 2014).

The processes on these two scales can be connected by understanding the structure and dynamics of the urban boundary layer (UBL), which is the lowest part of the troposphere in which surface-atmosphere exchanges occur that directly affect human activity. There have been a large number of numerical studies performed to improve our understanding of UBL processes during extreme heat events, which have been important for conceptualizing the role of synoptic-scale and surface forcings on urban climate. However, in-depth observational analyses of UBL structure and dynamics are limited, which has

This study attempts to use observations and analytical methods to provide insight into the following questions:

1. How do UBL quantities, such as temperature and moisture, differ from the climatology during extreme heat events?
2. How do UBL structure and dynamics depart from the climatology during extreme heat events?
- 3.

2 Data collection and analysis

2.1 Study site

The UBL over New York City is observed and analyzed in this study. Observational data was captured at four locations within New York City (Table 1).

Table 1: Locations and details of observations sites.

	Bronx	Manhattan	Queens	Staten Island
Coordinates	40.87248°N, -73.89352°E	40.82044°N, -73.94836°E	40.73433°N, -73.81585°E	40.60401°N, -74.14850°E
Elevation (m a.g.l.)	57.8	90.6	56.3	32.4
Element roughness height (m a.g.l.)				
Instruments used	Lidar, microwave radiometer	Lidar, sonic anemometer	Lidar, radiometer, sonic anemometer	Lidar, microwave radiometer, sonic anemometer
Valid wind directions	N/A	120 to 300°	180 to 360°	None

2.2 Observational instruments

Observations of the UBL were made using a synthesis of microwave radiometers, lidars, sonic anemometers, and surface weather stations.

Vertical profiles of temperature and vapor density were captured using microwave radiometers (Radio-metrics MP-3000A). Profiles are captured at 58 height levels starting at 50 m and ending at 10 km above

60 ground level, with vertical steps of 50 m from 50 to 500 m, 100 m from 500 m to 2 km, and 250 m steps
61 above 2 km.

62 **2.2.1 Data availability**

63 **2.3 Derived quantities**

64 **3 Results**

65 **3.1 Normal and extreme heat boundary layer properties**

66 This section discusses the differences in boundary layer structure and properties between normal days
67 and extreme heat events. Results are presented from the averages over all identified normal and heat
68 event days.

69 **3.1.1 Temperature**

70 On average, extreme heat events increase the temperature at the surface, as expected (see Figure 3). This
71 is consistent across all observed locations in New York City, with the extreme heat event temperature
72 exceeding normal temperatures by approximately $1-\sigma$ over the entire day. An increase in the difference is
73 observed during daytime hours, with the difference peaking in magnitude around 13:00 LST at the hottest
74 time of day. The surface temperature variability is significantly lower during heat events ($\sigma = 1.77 \text{ K}$)
75 than during normal temperatures ($\sigma = 4.57 \text{ K}$).

76 Above the surface, extreme heat events similarly increase the temperature significantly over the lowest
77 3 km of the troposphere (see Figure 9), with standardized anomalies of θ ranging from $\sigma = 0.88$ to 1.20 .
78 The largest temperature anomalies shift from the surface layer in the mornings to span the entirety of
79 the mixed layer. This is reflective of strong surface forcing resulting in convection through the surface
80 layer, as indicated by the formation of a late morning superadiabatic layer at all locations (Figures 4, 5,
81 6).

82 The vertical profiles of θ suggests a degree of spatial variability exists between locations. One instance of
83 this spatial variability is vertical mixing; the Bronx site appears to have stronger vertical mixing based
84 on Figure 4, as θ remains constant for a greater height than at the Queens and Staten Island locations.
85 This phenomenon is more pronounced during extreme heat events, as a distinct mixed layer is apparent
86 in the Bronx during early (12:00 LST) and late (18:00 LST) afternoon hours. While the mixed layer
87 is also visible for the other locations, the strength of the mixed layer is emphasized by the negative $\frac{d\theta}{dz}$
88 values between 1000 and 1500 m.

89 **3.1.2 Moisture**

90 On average, extreme heat events increase the moisture at the surface, as indicated by the diurnal profiles
91 of specific humidity (q) (see Figure 7). This is also consistent across all observed locations in New
92 York City, with the extreme heat event temperature exceeding normal temperatures by approximately
93 $1-\sigma$ over the entire day. Although a distinct diurnal profile exists (q decreases during daytime hours),
94 the diurnal range is smaller in magnitude than temperature. It is also worth noting that the diurnal
95 range is lower for Staten Island than for the Bronx or Queens, suggesting that degree of urbanization
96 has a negative correlation with a diurnal range of q . Similar to surface temperature, the variability of
97 q is significantly lower during heat events ($\sigma = 2.14 \times 10^{-3} \text{ kg kg}^{-1}$) than during normal temperatures
98 ($\sigma = 3.18 \times 10^{-3} \text{ kg kg}^{-1}$).

99 **3.2 Effects of the sea breeze circulation**

100 **4 Discussion**

101 **5 Conclusions**

102 **References**

- 103 Anderson, G Brooke and Michelle L Bell (2011). “Heat waves in the United States: mortality risk during heat
104 waves and effect modification by heat wave characteristics in 43 US communities”. In: *Environmental health
105 perspectives* 119.2, pp. 210–218.
- 106 Black, Emily et al. (2004). “Factors contributing to the summer 2003 European heatwave”. In: *Weather* 59.8,
107 pp. 217–223.
- 108 Burillo, Daniel et al. (2019). “Electricity infrastructure vulnerabilities due to long-term growth and extreme heat
109 from climate change in Los Angeles County”. In: *Energy Policy* 128, pp. 943–953.
- 110 Chen, Feng, Xuchao Yang, and Weiping Zhu (2014). “WRF simulations of urban heat island under hot-weather
111 synoptic conditions: The case study of Hangzhou City, China”. In: *Atmospheric research* 138, pp. 364–377.
- 112 Forzieri, Giovanni et al. (2018). “Escalating impacts of climate extremes on critical infrastructures in Europe”.
113 In: *Global environmental change* 48, pp. 97–107.
- 114 Frumkin, Howard (2016). “Urban sprawl and public health”. In: *Public health reports*.
- 115 Heaviside, Clare, Helen Macintyre, and Sotiris Vardoulakis (2017). “The urban heat island: implications for health
116 in a changing environment”. In: *Current environmental health reports* 4.3, pp. 296–305.
- 117 Hu, Xiao-Ming and Ming Xue (2016). “Influence of synoptic sea-breeze fronts on the urban heat island intensity
118 in Dallas–Fort Worth, Texas”. In: *Monthly Weather Review* 144.4, pp. 1487–1507.
- 119 Jiang, Shaojing et al. (2019). “Amplified urban heat islands during heat wave periods”. In: *Journal of Geophysical
120 Research: Atmospheres* 124.14, pp. 7797–7812.
- 121 Li, Dan and Elie Bou-Zeid (2013). “Synergistic interactions between urban heat islands and heat waves: The
122 impact in cities is larger than the sum of its parts”. In: *Journal of Applied Meteorology and Climatology* 52.9,
123 pp. 2051–2064.
- 124 Madrigano, Jaime et al. (2015). “A case-only study of vulnerability to heat wave-related mortality in New York
125 City (2000–2011)”. In: *Environmental health perspectives* 123.7, pp. 672–678.
- 126 McEvoy, Darryn, Iftekhar Ahmed, and Jane Mullett (2012). “The impact of the 2009 heat wave on Melbourne’s
127 critical infrastructure”. In: *Local Environment* 17.8, pp. 783–796.
- 128 Miralles, Diego G et al. (2014). “Mega-heatwave temperatures due to combined soil desiccation and atmospheric
129 heat accumulation”. In: *Nature geoscience* 7.5, pp. 345–349.
- 130 Peng, Roger D et al. (2011). “Toward a quantitative estimate of future heat wave mortality under global climate
131 change”. In: *Environmental health perspectives* 119.5, pp. 701–706.
- 132 Ramamurthy, P and E Bou-Zeid (2017). “Heatwaves and urban heat islands: a comparative analysis of multiple
133 cities”. In: *Journal of Geophysical Research: Atmospheres* 122.1, pp. 168–178.
- 134 Stéfanon, Marc et al. (2014). “Soil moisture-temperature feedbacks at meso-scale during summer heat waves over
135 Western Europe”. In: *Climate dynamics* 42.5, pp. 1309–1324.
- 136 Zhao, Lei et al. (2018). “Interactions between urban heat islands and heat waves”. In: *Environmental research
137 letters* 13.3, p. 034003.
- 138 Zuo, Jian et al. (2015). “Impacts of heat waves and corresponding measures: a review”. In: *Journal of Cleaner
139 Production* 92, pp. 1–12.

140 **Appendix**

Table 2: Symbols and abbreviations used in the paper.

¹⁴¹

Symbol/Abbreviation	Definition
σ	Standard deviation
θ	Potential temperature
q	Specific humidity
UBL	Urban boundary layer
MLH	Mixed layer height

¹⁴² **Figures**

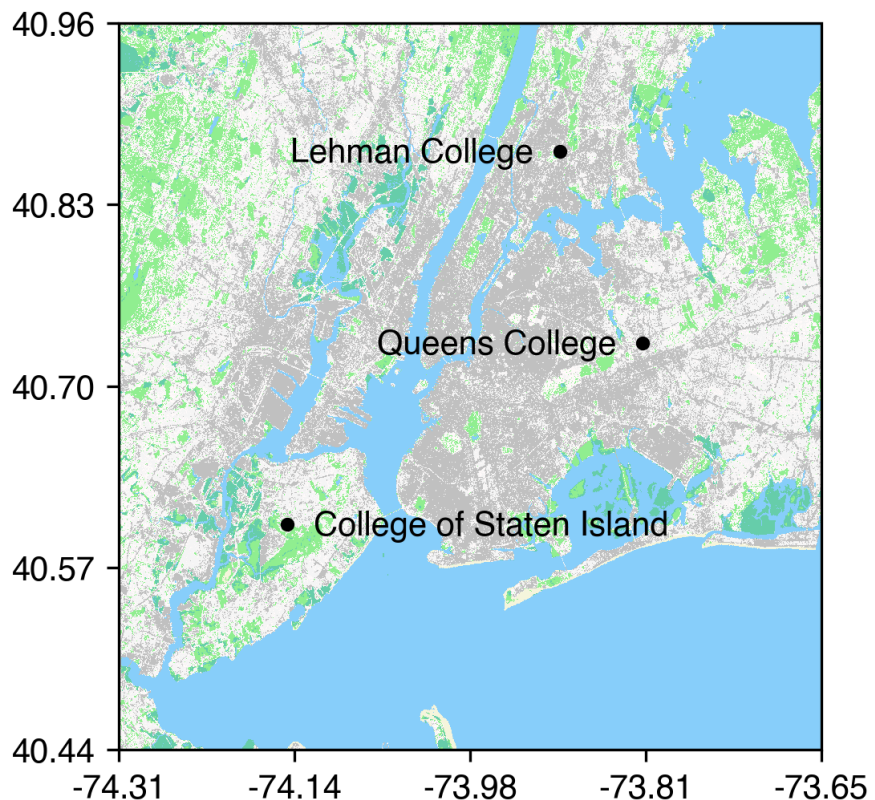


Figure 1: .

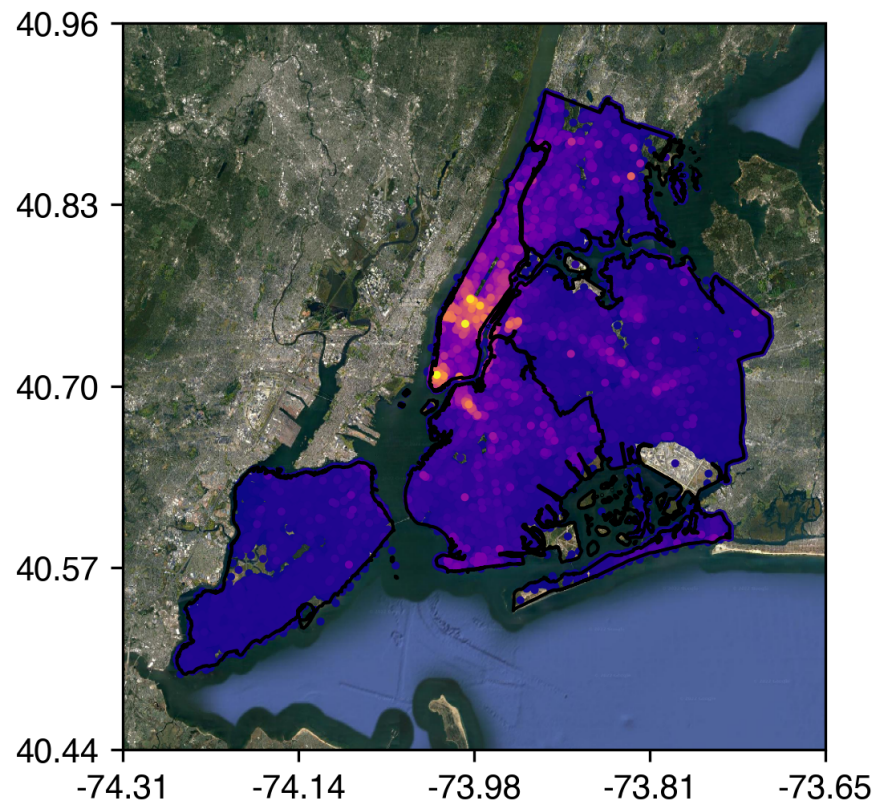


Figure 2: .

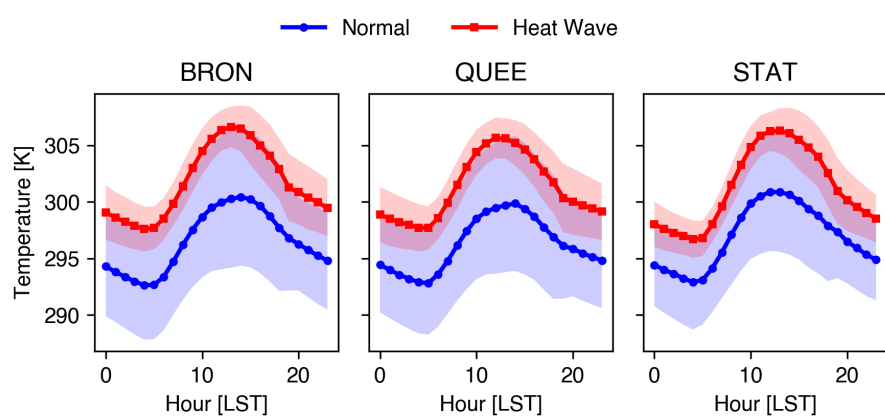


Figure 3: .

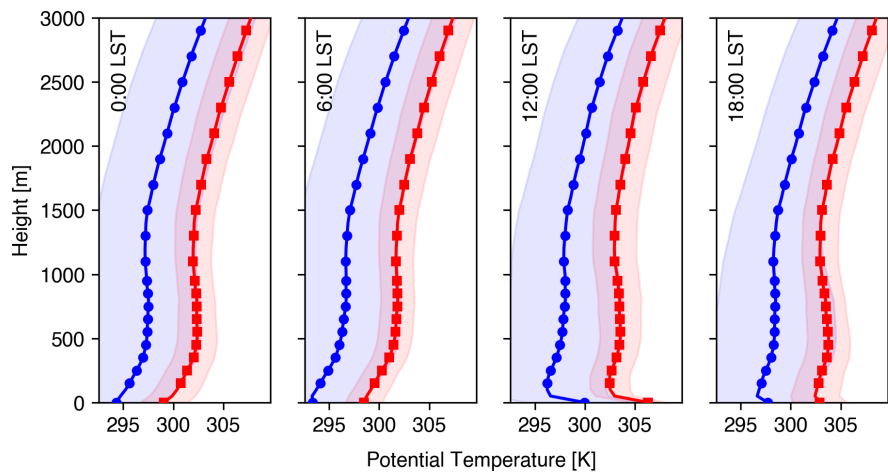


Figure 4: .

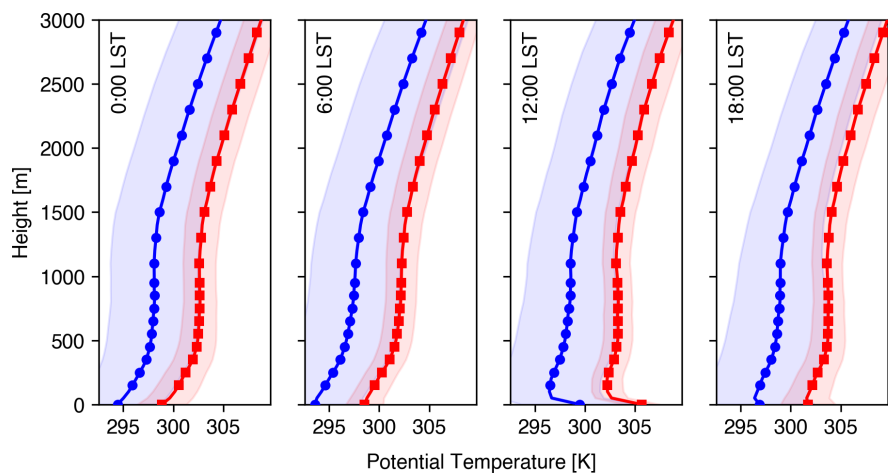


Figure 5: .

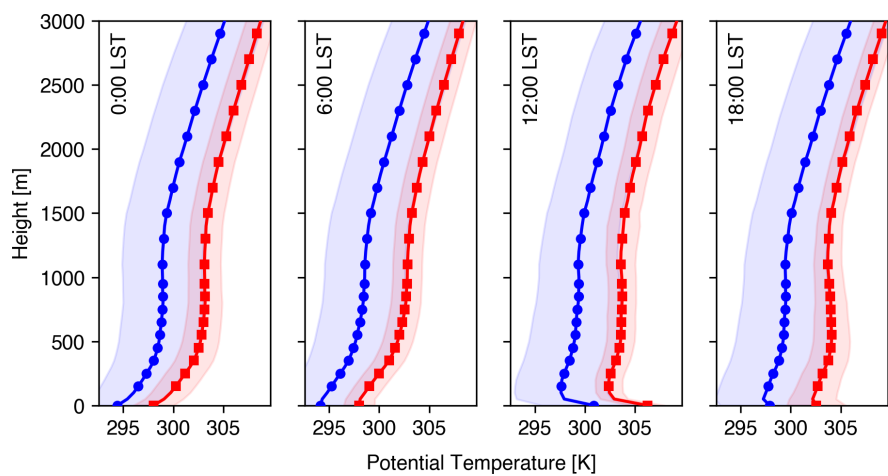


Figure 6: .

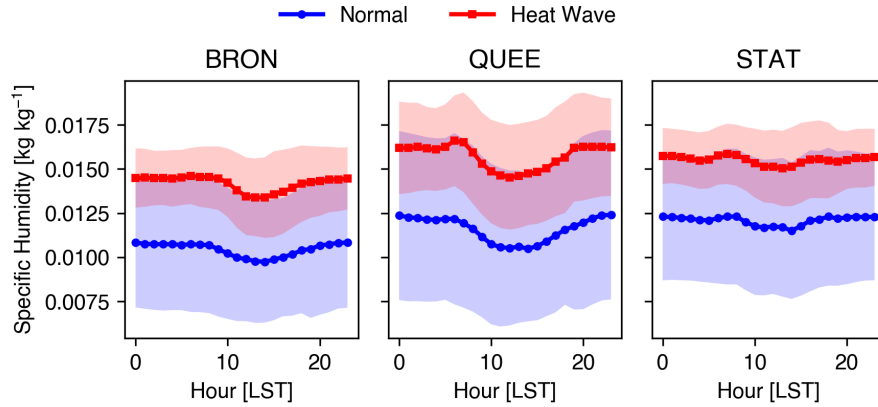


Figure 7: .

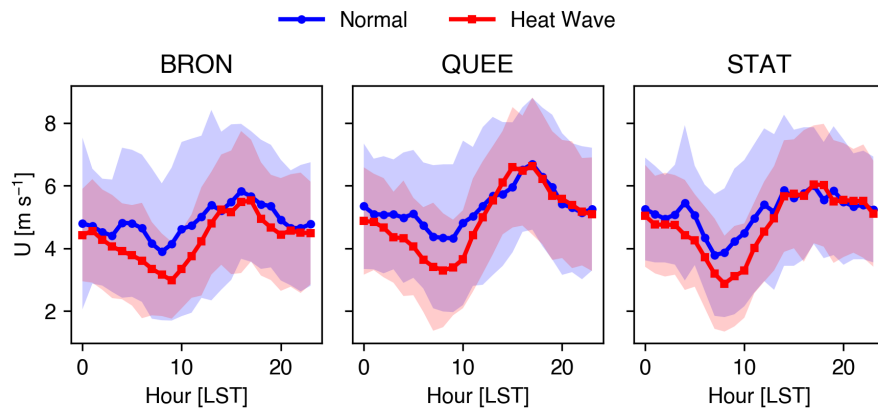


Figure 8: .

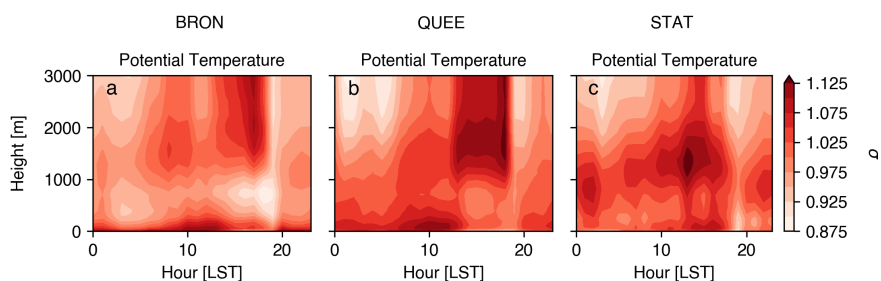


Figure 9: .

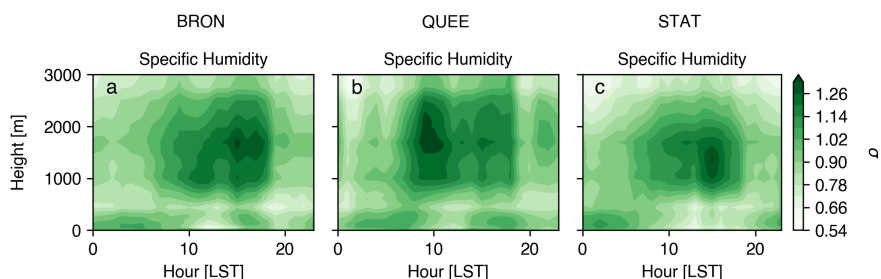


Figure 10: .

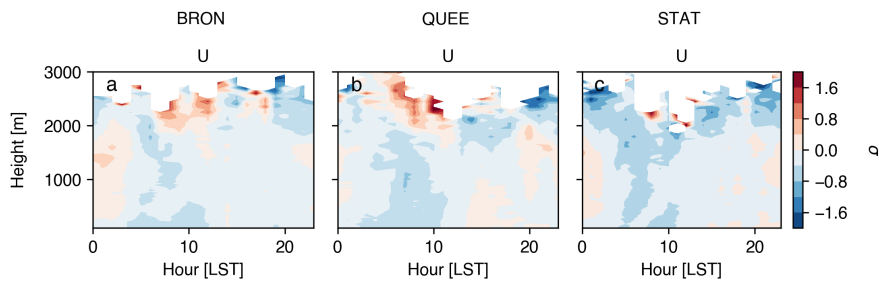


Figure 11: .

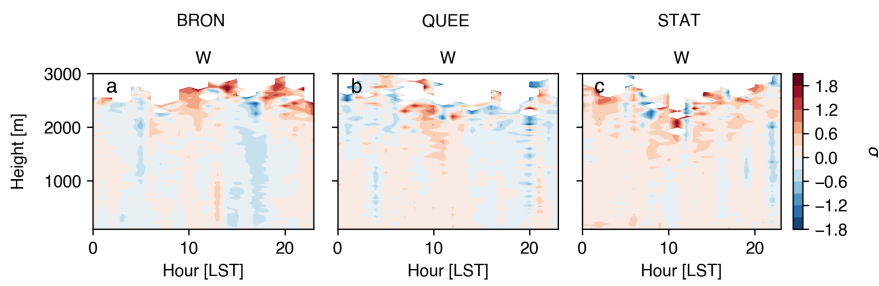


Figure 12: .

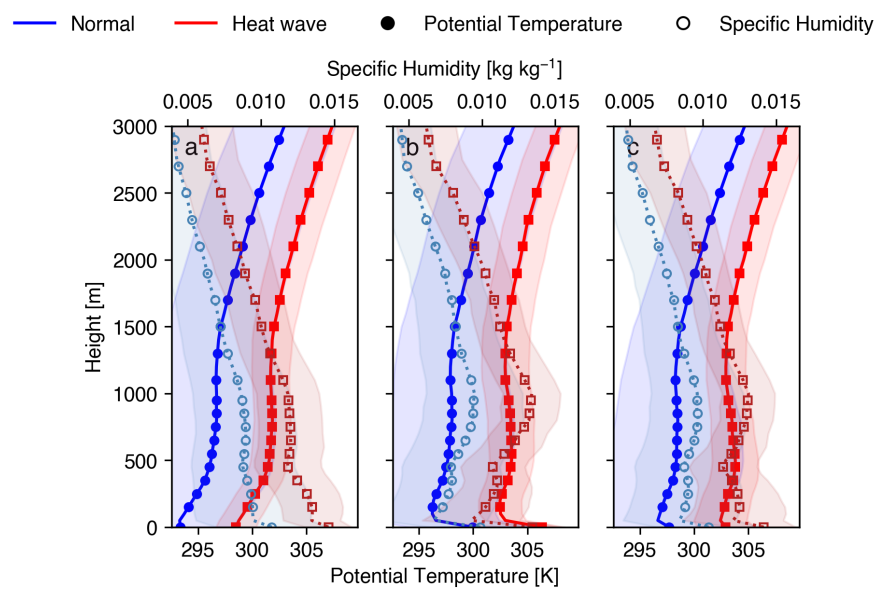


Figure 13: .

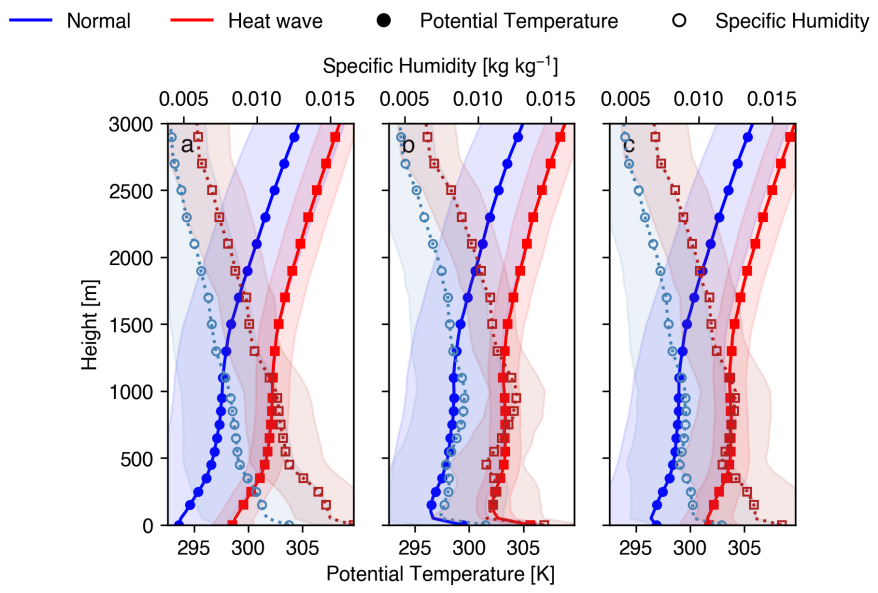


Figure 14: .

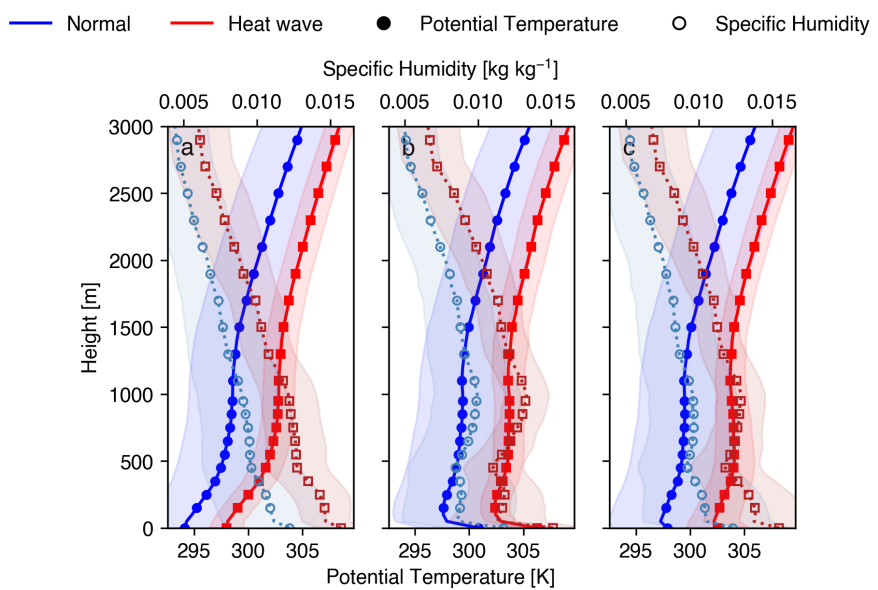


Figure 15: .

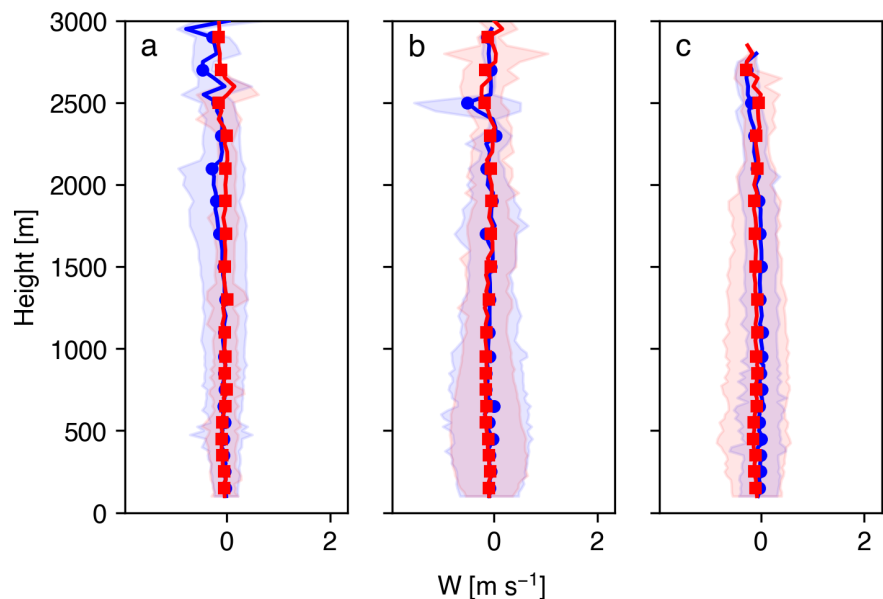


Figure 16: .

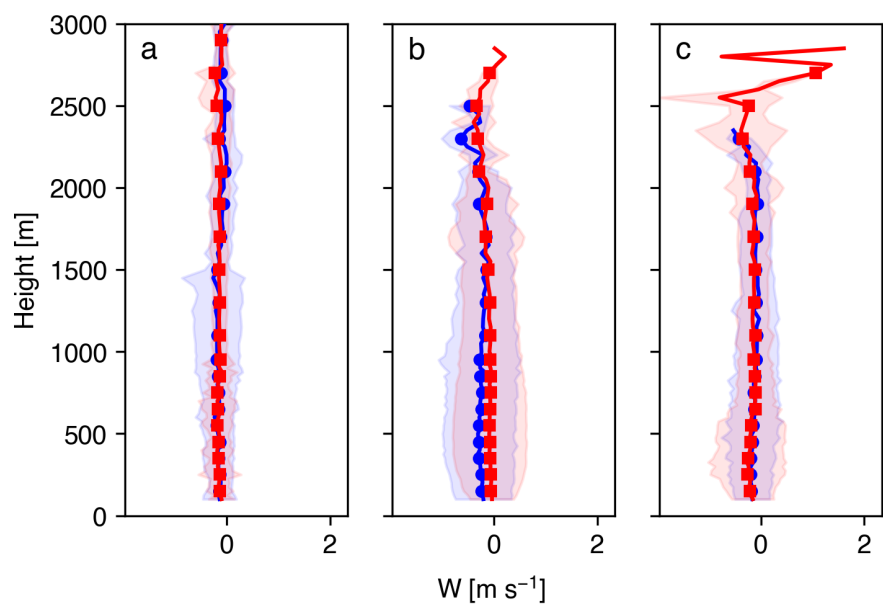


Figure 17: .

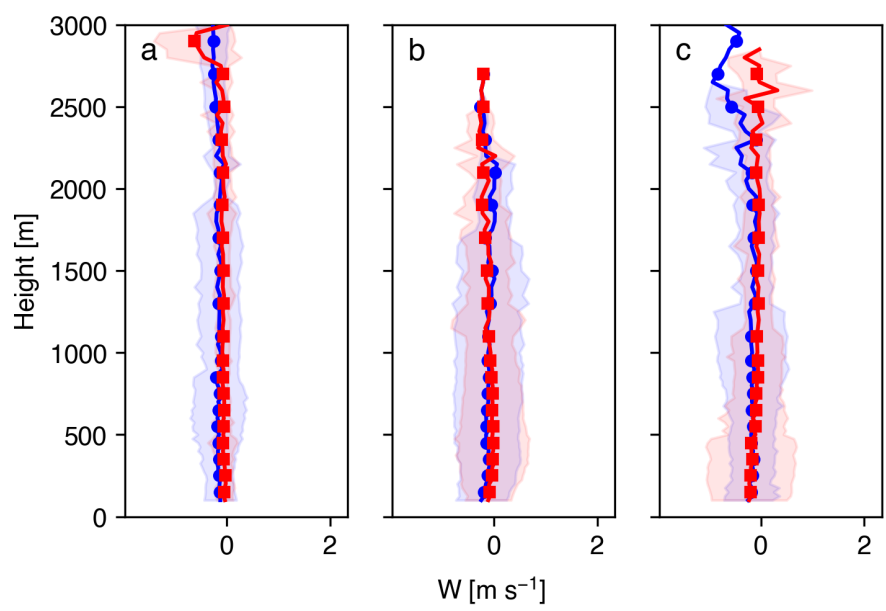


Figure 18: .

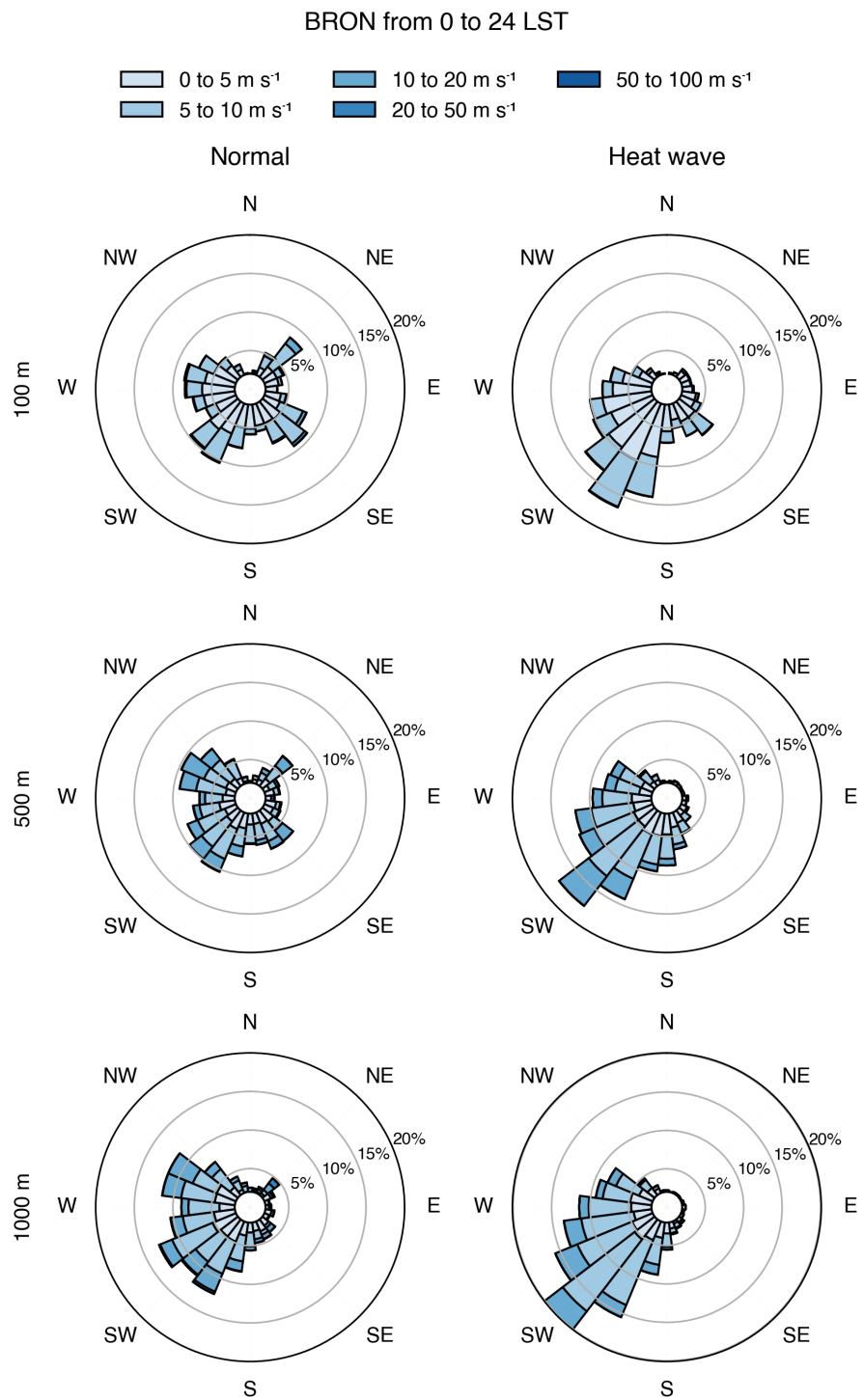


Figure 19: .

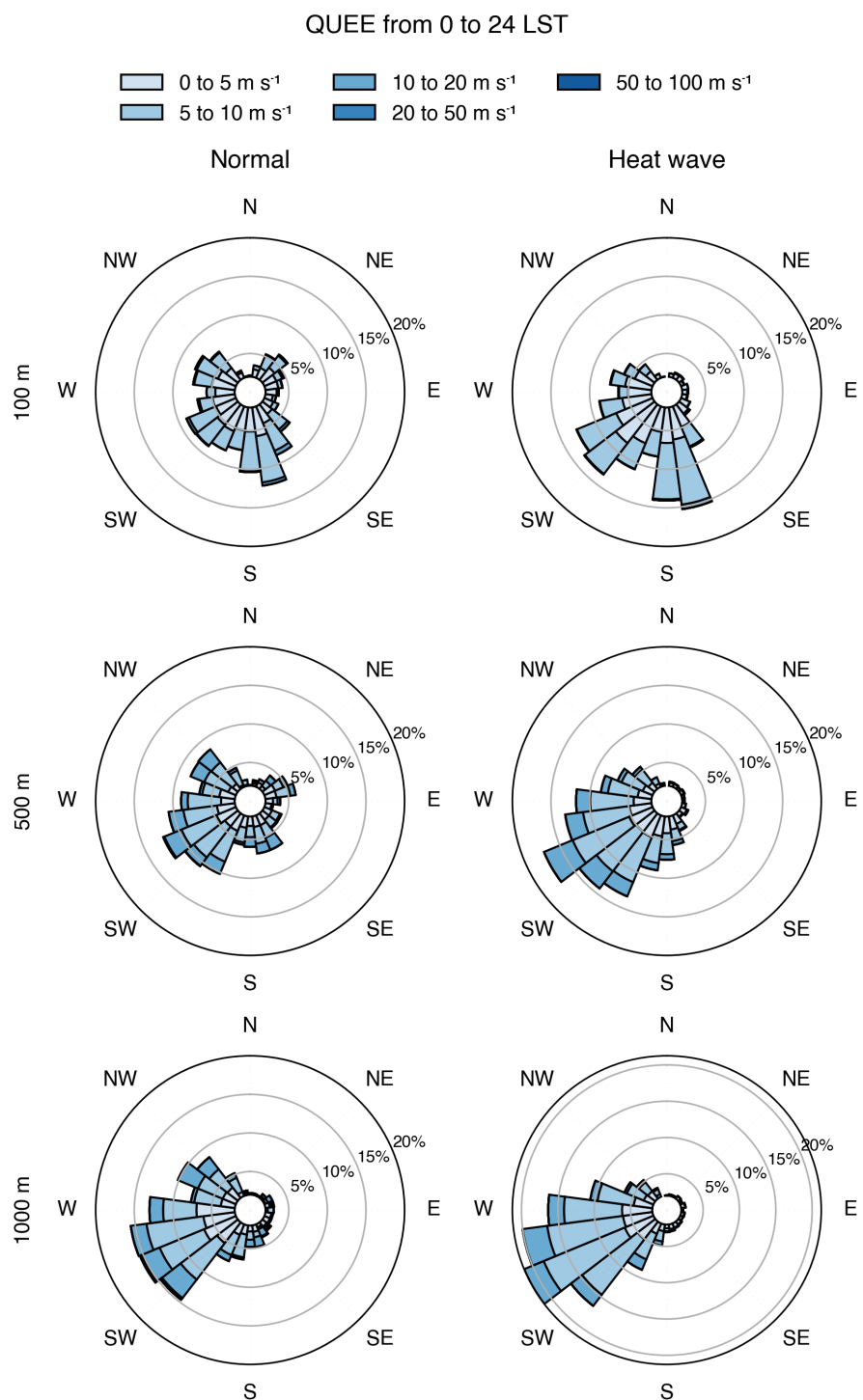


Figure 20: .

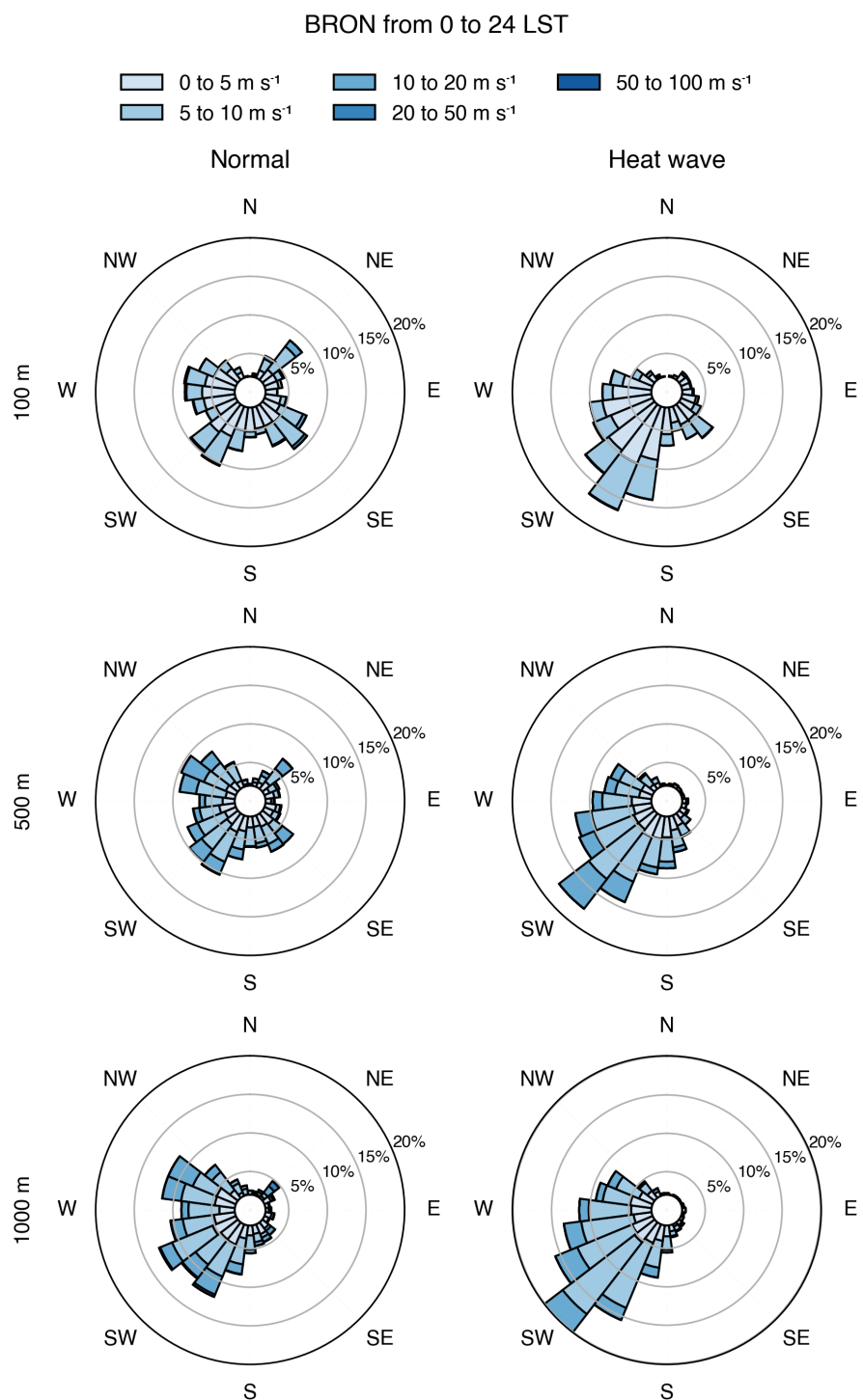


Figure 21: .